NASA TECHNICAL NOTE

NASA TN D-6783

EXPERIMENTAL INVESTIGATION OF AN AXISYMMETRIC FREE JET WITH AN INITIALLY UNIFORM VELOCITY PROFILE

by Thomas L. Labus and Eugene P. Symons

Lewis Research Center
Cleveland, Ohio 44135

NATIONAL AERONAUTICS AND SPACE ADMINISTRATION • WASHINGTON, D. C. • MAY 1972

1. Report No. NASA TN D-6783	2. Government Accession No.	3. Recipient's Catalog No.
4. Title and Subtitle EXPERIMENTAL INVESTIGATION OF AN AXISYMMETRIC FREE JET WITH AN INITIALLY UNIFORM VELOCITY PROFILE		5. Report Date May 1972 6. Performing Organization Code
7. Author(s) Thomas L. Labus and Eugene P. Symons		8. Performing Organization Report No. E-6801
9. Performing Organization Name and Address Lewis Research Center National Aeronautics and Space Administration Cleveland, Ohio 44135		10. Work Unit No. 113-31 11. Contract or Grant No.
12. Sponsoring Agency Name and Address National Aeronautics and Space Administration Washington, D.C. 20546		13. Type of Report and Period Covered Technical Note 14. Sponsoring Agency Code
15. Supplementary Notes		

16. Abstract

An experimental investigation was conducted to determine the flow characteristics of a circular free helium jet having an initially uniform velocity profile. Complete velocity profiles are presented at Reynolds numbers of 1027 and 4571 at 0, 3, 6, 10, 15, and 20 nozzle diameters (where possible) from the nozzle exit. Centerline velocity decay and potential-core length were obtained over a range of Reynolds numbers from 155 to 5349 at distance up to and including 25 nozzle diameters from the nozzle exit. Also presented are the angles of spread associated with the diffusion of the jet downstream of the nozzle. Axial jet momentum flux and entrained mass flux, at various distances downstream of the nozzle, are presented as a function of the jet Reynolds number.

17. Key Words (Suggested by Author(s))
Free jets
Fluid flow
Circular jet
Uniform profile

18. Distribution Statement
Unclassified - unlimited

19. Security Classif. (of this report)	20. Security Classif. (of this page)	21. No. of Pages	22. Price*
Unclassified	Unclassified	23	$3.00

* For sale by the National Technical Information Service, Springfield, Virginia 22151

EXPERIMENTAL INVESTIGATION OF AN AXISYMMETRIC FREE JET WITH AN INITIALLY UNIFORM VELOCITY PROFILE

by Thomas L. Labus and Eugene P. Symons

Lewis Research Center

SUMMARY

An experimental investigation was conducted to determine the flow characteristics of a circular free helium jet having an initially uniform velocity profile. Complete velocity profiles are presented at Reynolds numbers of 1027 and 4571 and 0, 3, 6, 10, 15, and 20 nozzle diameters (where possible) from the nozzle exit. Centerline velocity decay and potential-core length were obtained over a range of Reynolds numbers from 155 to 5349 at distances up to and including 25 nozzle diameters from the nozzle exit. Also presented are the angles of spread associated with the diffusion of the jet downstream of the nozzle. Axial jet momentum flux and entrained mass flux, at various distances downstream of the nozzle, are presented as a function of the jet Reynolds number.

INTRODUCTION

A thorough knowledge of the dynamics of various types of low-speed jet flow is required for many engineering applications. Some of these include the extensive area of fluid amplifiers, liquid inflow and vapor impingement in weightlessness and near weightlessness, and the laminar gas jet diffusion flame. The prediction of the interaction of a jet with any object necessitates a basic understanding of the flow characteristics of the jet itself. The area of incompressible low-speed jets is further complicated by the fact that the jet behavior varies in different regions as a function of the jet Reynolds number. Also, the jet characteristics are dependent on such factors as the internal shape of the nozzle from which the jet exits, the region or environment into which the jet enters, the initial velocity profile of the jet at the nozzle exit, the orientation of the jet with respect to the gravity vector, and even the external shape of the nozzle. A survey of the available literature on jet flow indicates that many of these factors (Reynolds number, internal and external nozzle shape, orientation, and environment) have not been specifically

discussed. A knowledge of the mass or volumetric flow rate through a nozzle alone is insufficient to fully describe the subsequent downstream jet behavior.

The only known analytical result for a three-dimensional laminar free jet is that attributed to Schlichting (ref. 1). A similarity solution for the velocity profile downstream of the nozzle exit was obtained by employing the three-dimensional Navier-Stokes equations, taking symmetry into account, and using boundary layer assumptions. The major disadvantage with Schlichting's analytical solution is that the jet is assumed to exit from an infinitesimally small aperture and, thus, cannot be expected to be representative of experiment data except at very large distances from the nozzle.

Experimental results for both laminar and turbulent free jets exiting from a circular aperture can be found in references 2 to 9. References 2 and 8 are specifically concerned with the flow characteristics of a circular, uniform, free jet exiting into a constant pressure region. The lowest Reynolds number for uniform jets at which the centerline velocity decay and associated potential-core length have been investigated is 600 (ref. 8). Angles of spreading have been investigated for uniform jet Reynolds numbers of 22 000 and above (ref. 2). Since a slight discrepancy exists between these works, they are discussed in more detail in the section entitled BACKGROUND INFORMATION.

The purpose of this report is to present the results of an experimental investigation conducted at the NASA Lewis Research Center to study the flow characteristics of a circular, uniform (flat profile), free jet exiting into a constant pressure region.

Helium was employed both as the jet and as the environment into which the jet exited. The external shape of the experiment nozzle was that of a tube, and the axis of the nozzle was oriented vertically upward.

This investigation extended the lower limit of jet Reynolds number investigated to 155 (based on nozzle diameter) for potential-core length and to 468 for angles of spreading. The complete velocity profiles were measured at 0, 3, 6, 10, 15, and 20 nozzle diameters at two specific Reynolds numbers. The centerline velocity decay and the angle of jet spreading were obtained at various Reynolds numbers between 155 and 5349. The axial jet momentum and entrained mass flux are presented as functions of the jet Reynolds number. Comparisons of the centerline velocity decay and the angle of spread of the jet were made with the experimental results obtained from references 2 and 8.

SYMBOLS

D internal diameter of nozzle, cm

H axial distance from nozzle, cm

M momentum flux, N

M_o momentum flux at nozzle exit, N

$\dot{m}$ mass flow rate, g/sec

$\dot{m}_o$ mass flow rate at nozzle exit, g/sec

P_D dynamic pressure, N/cm^2

P_s static pressure, N/cm^2

P_t total pressure, N/cm^2

R internal radius of nozzle, cm

Re jet Reynolds number, $\rho U_{max} D/\mu$

r radial distance, cm

r_j radial distance to jet edge, cm

r_o radial distance at nozzle exit, cm

U_{cl} jet centerline velocity, cm/sec

U_{max} maximum axial velocity at nozzle exit, cm/sec

U_x axial jet velocity, cm/sec

θ_1 half-angle of spread in region of flow establishment, deg

θ_2 half-angle of spread in region of established flow, deg

μ viscosity, $(N)(sec)/cm^2$ (1.94×10^{-9} at 20^o C for helium)

ρ density, g/cm^3 (0.1663×10^{-3} at 20^o C for helium)

BACKGROUND INFORMATION

Since the general category of jet flow is so extensive, a wide variety of reports and papers as well as several books have been written on the subject. For purposes of simplification, only three representative reports, each dealing with flow characteristics of axially symmetric free jets having a uniform velocity profile at the nozzle exit are discussed herein.

Reference 7 contains an excellent description of the flow regimes which exist downstream of the nozzle for a jet having a uniform velocity profile at the nozzle exit. The initial region is termed the region of flow establishment and extends from the nozzle exit to the apex of the potential core. (The potential core is the region in the jet in which the centerline velocity remains essentially constant and equal to the centerline velocity at the nozzle exit.) The second region is termed the region of established flow. This

region begins at the end of the potential core and is characterized by a gradual, but appreciable, decay in the centerline velocity.

Reference 7 states that there are four characteristic jet patterns for free jets: dissipated laminar, fully laminar, semiturbulent, and turbulent. For any given nozzle geometry, these types of jets should be a function of the jet Reynolds number. However, due to slight differences in nozzle design, no distinct value of jet Reynolds number can be used to define the end of one type of jet and the beginning of another for all nozzles.

As discussed in the INTRODUCTION, references 2 and 8 are specifically concerned with the flow characteristics of a circular, uniform, free jet exiting into a constant pressure region. Reference 2 reports the results of an experimental and analytical investigation. Air was employed as the working fluid and Reynolds numbers of 22 000 and above (based on nozzle diameter) were examined. Various measurement techniques were employed in reference 2. For nozzle exit velocities and for velocities in the near vicinity of the nozzle exit, a hypodermic needle connected to a differential water manometer was used. A micromanometer was employed for moderate velocities. For low velocities, a midget spoke-vane anemometer was employed. At very low jet velocities, a fine jet of smoke was used for visual observation. The major conclusions obtained were that the potential-core length was 6.2 nozzle diameters, independent of the Reynolds number, and that the half-angle of spreading was 6° to 8° in the region of flow establishment and 10° to 12° in the region of established flow, also independent of the Reynolds number.

In reference 8, an experimental investigation of the dynamic characteristics of a circular free jet with an initially uniform velocity profile was conducted. Air was employed as the working fluid and jet Reynolds numbers, based on nozzle diameter, ranged from 600 to 100 000. For large velocities, a U-tube mercury manometer was used; for low jet velocities, measurements were taken with a micromanometer. The major conclusions of reference 8 are as follows: The potential-core length increased as the nozzle exit Reynolds number increased through the laminar range and reached a maximum at a Reynolds number of 1000 (approximately 21 nozzle diameters). The potential-core length abruptly decreased as the nozzle exit Reynolds numbers increased beyond 1000, reached a minimum, and then increased only slightly up to a value of about 10 000. For values greater than 10 000, the potential-core length was found to be essentially independent of the nozzle exit Reynolds number and equal to 6.1. The authors of reference 8 did not examine the angle of spread extensively, but did show fair agreement with the results of reference 2 at high Reynolds numbers.

APPARATUS

Selection of Experiment Nozzle and Gas

Part of the objective of this study was to examine the flow characteristics of a circular, uniform, free jet at low Reynolds numbers. An examination of the parameters in the Reynolds number $\rho U_{max} D/\mu$ indicates that, for a constant jet Reynolds number, the largest velocity would be obtained by minimizing the nozzle diameter and maximizing the kinematic viscosity μ/ρ. These values, of course, must be chosen with some practicality for, if the nozzle diameter was chosen too small in relation to the pressure probe, it would be impossible to obtain enough data to define a velocity profile. As a result of these considerations, helium was chosen as the working gas, and a nozzle diameter of 0.254 centimeter (0.1 in.) was selected.

Experiment Hardware

The experiment apparatus employed in this study is shown in figure 1. The major components of this system are described in the following sections.

Test chamber. - As shown in figure 1, the test chamber consisted of a plastic section having a hemispherical top (93.98 cm in diam), a cylindrical section (41.91 cm high),

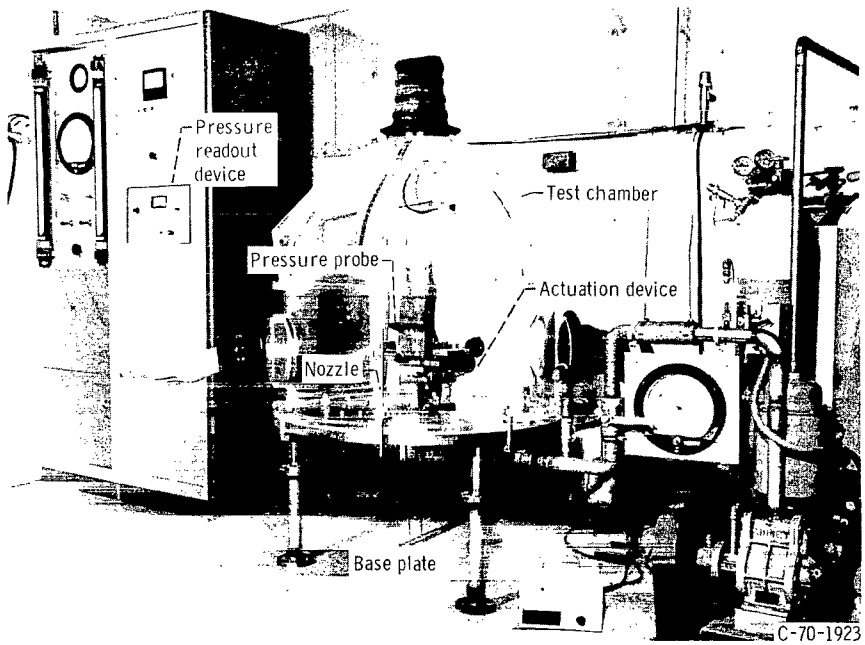

Figure 1. - Experiment apparatus.

and a stainless-steel base plate (93.98 cm in diam). The plastic section was fabricated as one unit and had three ports, circular in shape, with flanges attached so as to be compatible with the neoprene gloves and accordian sleeves which were used for access to the components within the chamber. This dome was fastened to the base plate at six locations by the use of knurled nuts, and a positive seal was obtained by means of an O-ring. The dome was transparent so that visual observation of the apparatus contained within the dome was possible.

Base plate and supporting structure. - The stainless-steel base plate was supported by three cylindrical legs which were in turn securely anchored to a concrete floor to eliminate the disturbing influences of vibrations which could be transmitted to the jet. The legs were equipped with leveling jacks, and the base plate could thus be alined by using a precision level capable of measuring deflections as small as 0.0083 centimeter per meter (0.001 in./ft). Hermetically sealed small circular ports in the base plate permitted connection of gas lines, vacuum lines, and pressure lines to the test chamber.

Actuation device. - The actuation device for varying the position of the pressure probe is shown in figure 2. This slide assembly consisted of three mutually perpendicular machined surfaces and thus permitted movement in three directions. Slide travel in the plate normal to the nozzle axis was precisely measured by two dial indicators accurate to within 0.00254 centimeter (0.001 in.), and vertical travel was measured to within 0.00508 centimeter (0.002 in.). The actuation device was attached to the stainless-steel

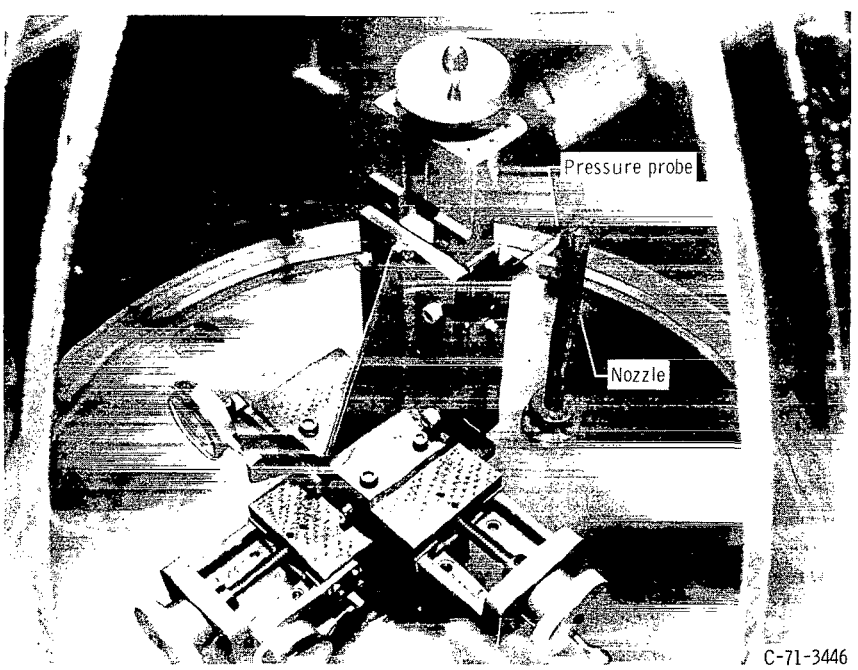

Figure 2. - Actuation device.

base plate by four screws, and each machined surface was leveled with respect to the base plate and to each of the other two surfaces.

Pressure readout device. - The precision pressure readout unit is shown mounted in the panel in figure 1. In order to obtain the dynamic pressure, a capsule acting as a pressure transducer and contained within the unit had two inlet ports, one connected to the total head pressure probe and the other connected to a static port located at the base plate. This location for the static pressure pickup was chosen since the authors were of the opinion that this location would provide the most accurate representation of the true static pressure existing in the jet. Most studies determine static pressure by means of a pickup located on the total head tube and positioned within the flow. In such a location, the indicated static pressure could conceivably be in error due to the effects of turbulence (ref. 10), compressibility (ref. 11), and pickup geometry (ref. 12). For example, Miller and Comings (ref. 10) found that static pressure measured within the flow at high jet Reynolds numbers (Re = 17 800) differed from ambient pressure. It is difficult to determine whether these observed trends were due to one of the previously mentioned effects or if they actually exist. Since the present study was conducted for fairly low jet Reynolds numbers (hence, incompressible flow), the effects of turbulence and compressibility were negligible; and in order to eliminate the effect of pickup geometry, the static pressure location on the base plate was selected. A gage, through the internal quartz Bourdon tube capsule, indicated the difference between the total and static pressures to provide a measure of the dynamic pressure of the jet. Through a procedure discussed in the section DATA ANALYSIS, the dynamic pressure was converted to a velocity measurement. Dynamic pressures as low as 1.15×10^{-1} newton per square meter (0.000017 psia) could be read with this device. This pressure reading corresponds to the axial velocity of 1.18 centimeters per second, which is, thus, the lowest value of velocity which could be resolved with the apparatus. It should be noted that the accuracy of the calculated velocity is a function of the reading of the pressure readout device, and the corresponding errors involved become insignificant as the magnitude of the reading increases.

Nozzle. - A drawing of the brass nozzle used in this investigation is shown in figure 3. A 30° convergent section at the outlet of the 0.254-centimeter-diameter nozzle,

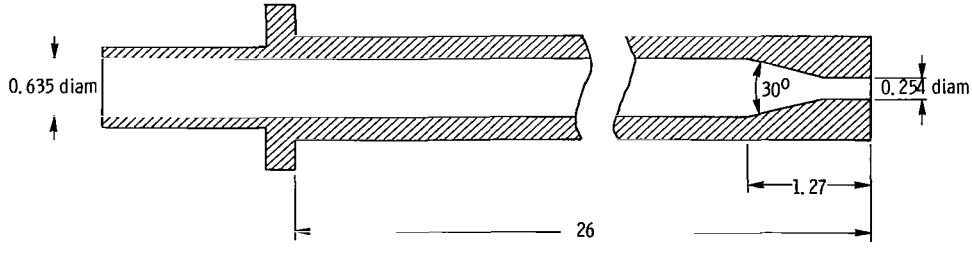

Figure 3. - Experiment nozzle (dimensions in centimeters).

having a well-rounded transition, was fabricated to provide a uniform velocity profile for the exiting helium jet. The nozzle, which was machined to very close tolerances, was fastened to a supporting structure on the base plate. This supporting structure had also been precisely machined and alined so as to ensure that the nozzle would be oriented normal to the base plate.

Pressure probe. - Pressure and thus velocity measurements of the helium jet were obtained with a total head pressure probe fabricated from stainless steel (see fig. 4).

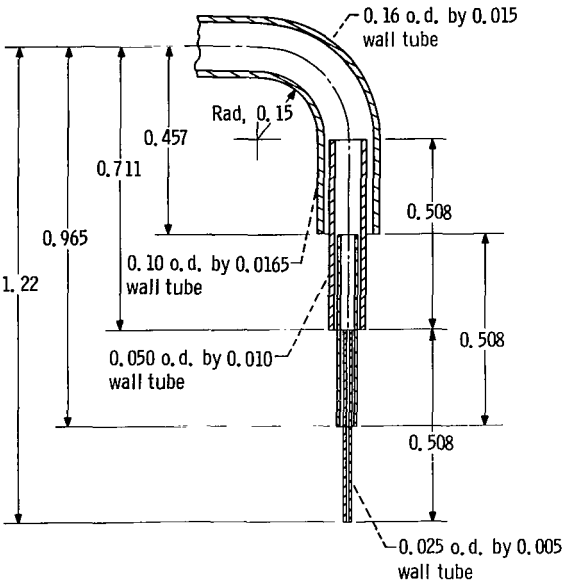

Figure 4. - Experiment pressure probe (dimensions in centimeters).

This probe was rigidly attached to the actuation device to assure that the axis of the probe was parallel to the axis of the nozzle. The opening at the end of the probe was circular and had a diameter of 0.015 centimeter (0.006 in.). The probe was sized to yield a reasonable time constant and was connected to a port located on the base plate by small-diameter plastic tubing.

OPERATING PROCEDURE

The flow schematic is shown in figure 5. The gas in the experiment test chamber was initially evacuated by means of the vacuum pump (shown in fig. 1) to a pressure of the order of 20 newtons per square meter (0.15 torr). In order to prevent the gloves

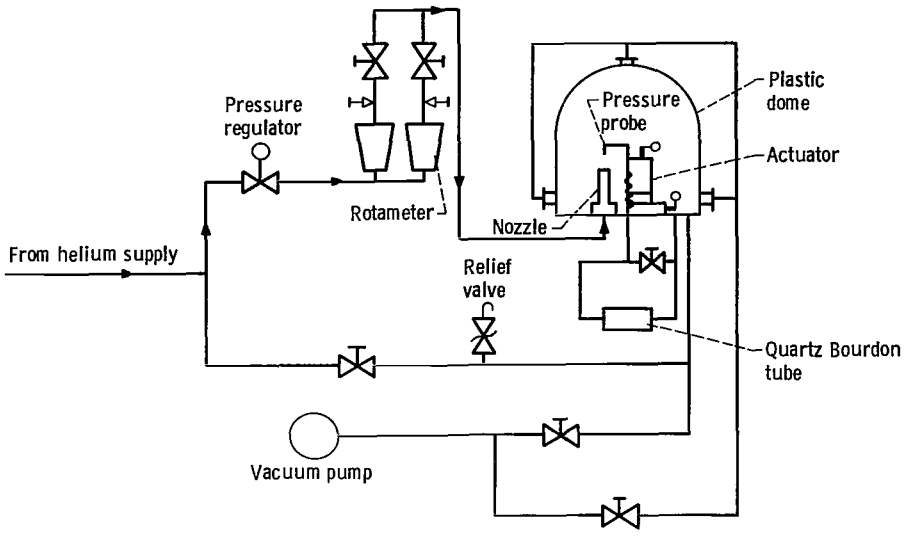

Figure 5. - Flow schematic.

from imploding, both sides of the gloves were evacuated by placing cover plates over the glove ports. The system was then filled with helium and again evacuated. This procedure was repeated four times in order to ensure that the environment in the test chamber was essentially pure helium before any measurements of the velocity profile were taken.

After the fourth pumpdown, helium was introduced into the test chamber until a positive pressure of 0.138×10^4 newtons per square meter (0.2 psi) above atmosphere was obtained in the chamber and the cover plates on the glove ports were removed. This pressure was maintained through the entire test by a pressure regulator and relief valve system and served to eliminate the danger of air leakage into the chamber.

Helium was then introduced into the chamber through the test nozzle by activating a series of pressure regulators and valves in series with one of the two available rotameters. The rotameters were chosen so that one would be used to measure higher mass flow rates and the other to measure lower mass flow rates. The temperature and the pressure of the helium were measured on gages located upstream of the rotameter. Thus, any necessary corrections due to these system variables would be made. The flow rate could be determined to an accuracy of ±4 percent by this system.

The determination of the jet centerline was made by pressure surveys across the jet at the nozzle exit. The highest pressure obtained indicated the location of the jet centerline. Once the centerline position was determined, surveys were taken across the jet using this point as a reference. Profiles were taken at distances of 0, 3, 6, 10, 15, and 20 nozzle diameters from the exit.

DATA ANALYSIS

The velocity distribution downstream of the nozzle exit was obtained from the measurement of the dynamic pressure as obtained from the precision pressure readout instrument. This instrument measured the difference between the total pressure associated with the incoming gas jet entering the probe and the static pressure as measured by means of a pressure tap located on the base plate. By employing Bernoulli's equation (conservation of energy along a streamline) between the point at which the jet velocity is desired and the point at which the gas jet comes to rest (i.e., the stagnation point), the total pressure can be calculated:

$$P_s + \frac{\rho U_x^2}{2} = P_t \tag{1}$$

The pressure readout instrument measures the difference between the total and static pressure, or the dynamic pressure:

$$P_D = \frac{\rho U_x^2}{2} \tag{2}$$

It is recognized that viscous forces at very low Reynolds numbers (based on the outside radius of the total head tube) can render Bernoulli's equation (as shown in eq. (1)) inapplicable and that a drag coefficient would be required for an accurate determination of the actual dynamic pressure P_D. (See ref. 13.) The net results of this consideration would be to reduce the actual velocity in the region near the periphery of the jet. Correction, if applied to the data presented in this report, would show a nearly negligible effect on the jet and, of course, no effect in the determination of the jet edge. Thus, equation (1) will be strictly adhered to herein.

From the manufacturer of the readout instrument, a chart of pressure difference and gage counter reading was furnished, and recalibration verified that the values given were correct. An equation for the pressure gage counter reading was developed and solved with the dynamic-pressure - velocity expression (eq. (2)). The simultaneous solution of these two equations, therefore, yielded the appropriate functional relation between the gas jet velocity and the gage counter reading.

RESULTS AND DISCUSSION

Establishment of Initially Uniform Velocity Profile

For a tube of variable cross-sectional area decreasing with distance toward the nozzle exit, it is known that boundary layer buildup can be minimized (ref. 14) and that a nearly uniform velocity profile can be achieved at the nozzle exit. Since the exact variation of cross section with both distance and jet Reynolds number is at present unknown, the nozzle employed was designed with 30^{o} convergent approach (see fig. 3).

The initial velocity profile H/D = 0 was obtained and compared in terms of uniformity at two Reynolds numbers. In figure 6, the dimensionless axial velocity as a

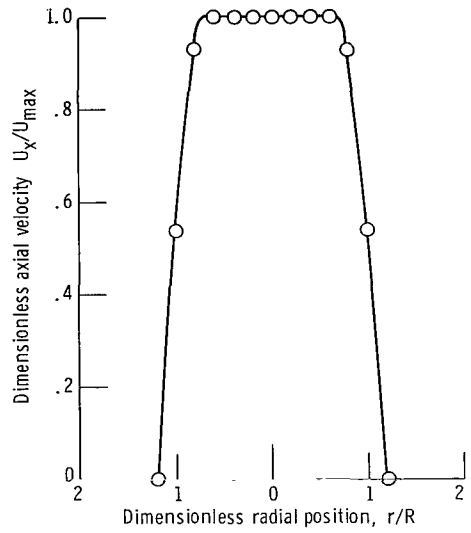

Figure 6. - Initial velocity profile shape - jet Reynolds number, 155.

function of dimensionless radial position is shown at a Re of 155. The jet was uniform to a r/R of 0.6, after which it decreased quite rapidly. Of the Reynolds numbers investigated, this is the worst possible case since the boundary layer thickness for the entrance region of a nonconverging tube is known to be inversely proportioned to $Re^{1/2}$ (ref. 15).

In figure 7, a similar plot is obtained for data taken at a Reynolds number of 4571. In this case, the jet remained uniform out to a dimensionless radial position of 0.8. It is noted that in both figures 6 and 7, the positions of zero jet velocity were not obtained at a nondimensional radial position of unity, since the experiment probe had an inside diameter of 0.015 centimeter (0.006 in.) and, as such, one-half of the probe (0.0076 cm (0.003 in.)) was actually positioned within the flow.

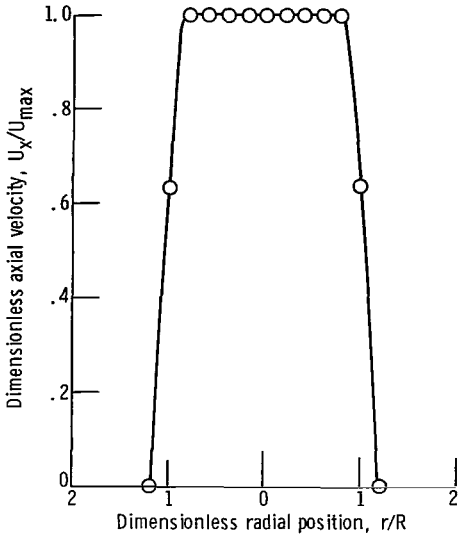

Figure 7. - Initial velocity profile shape - jet Reynolds number, 4571.

The profiles were more uniform at the higher Reynolds number than at the lower Reynolds number, as expected. At all Reynolds numbers intermediate to those presented in figures 6 and 7, the profiles are expected to be correspondingly intermediate.

Velocity Profiles Downstream of Nozzle

The complete velocity profiles for a Reynolds number of 1027 are shown in figure 8 at downstream distances H/D of 0, 3, 6, 10, 15, and 20 diameters from the nozzle exit. Examination of the radial positions in figure 8 where the axial jet velocity goes to zero indicates that the jet width does not increase rapidly as a function of H/D. As a result, measurements were obtained over the entire width of the jet for all values of H/D despite the knowledge that the jet should be axisymmetric. In figure 9, the complete velocity profiles for a Reynolds number of 4571 are shown at 0, 3, 6, 10, and 15 nozzle diameters downstream of the nozzle exit. It was impossible to obtain a complete velocity profile at an H/D of 20 due to experiment limitations in total probe travel. In figure 9, the jet width varies quite rapidly with increasing H/D. Therefore, measurements were taken over one-half of the profile; and symmetry was assumed, causing figure 9 to appear slightly more symmetric than figure 8. The data for these two Reynolds numbers show the large contrast which can occur between jets having initially uniform velocity profiles. The jet at the Reynolds number of 4571 is considerably wider than the low-Reynolds-number jet at an H/D of 15 (compare figs. 8(e) and 9(e)). Also, it can be seen that the centerline velocity has decayed quite dramatically at the higher Reynolds number.

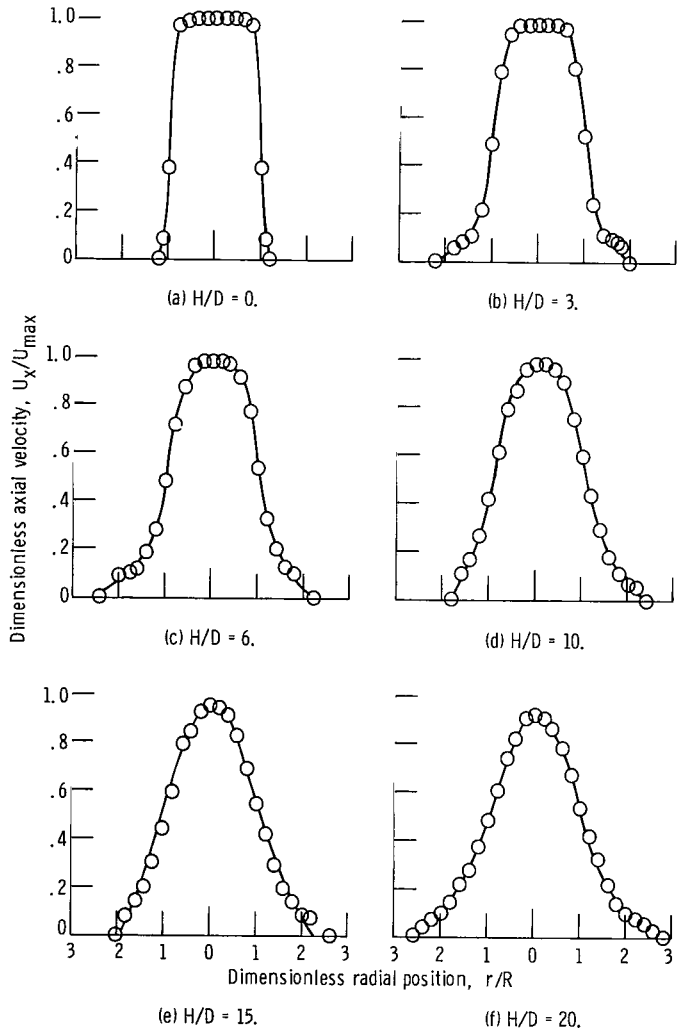

Figure 8. - Velocity profiles downstream of nozzle - jet Reynolds number, 1027. (H/D is ratio of axial distance from nozzle to internal diameter of nozzle.)

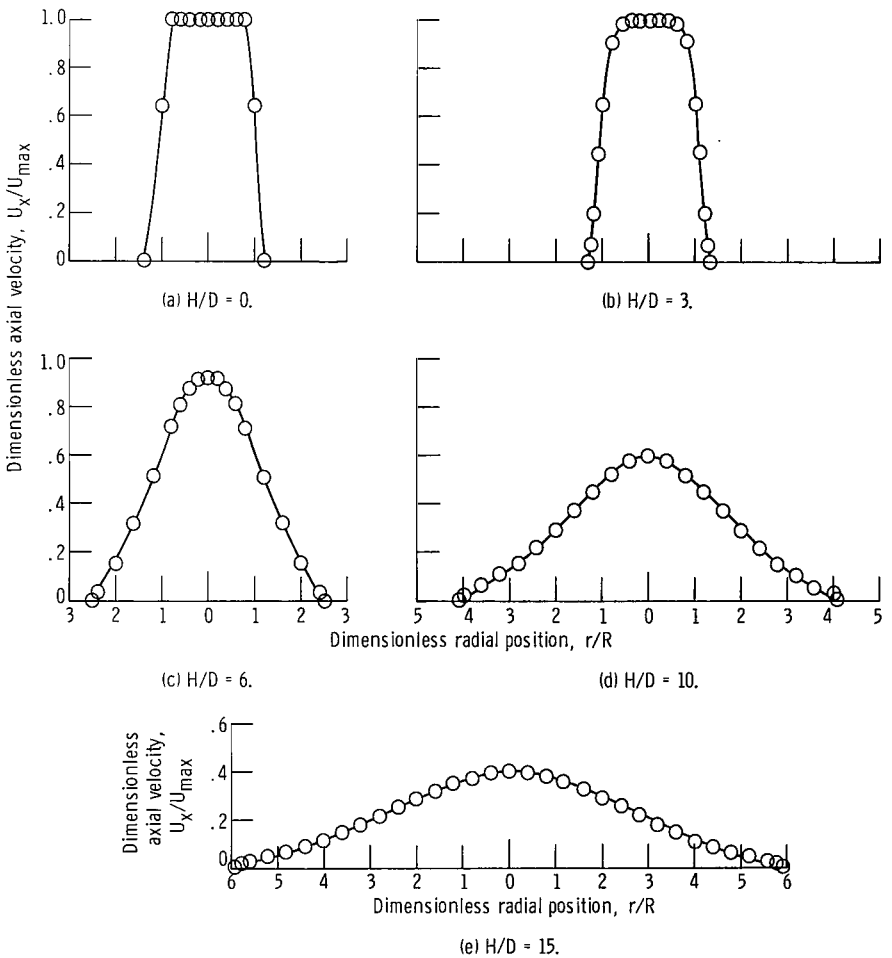

Figure 9. - Velocity profiles downstream of nozzle - jet Reynolds number, 4571. (H/D is ratio of axial distance from nozzle to internal diameter of nozzle.)

Conservation of Jet Momentum

The axial jet momentum flux at the nozzle exit for a jet having an initially uniform velocity profile is given by

$$M_o = \pi \rho r_o^2 U_{max}^2 \tag{3}$$

At any distance downstream of the nozzle exit, the axial jet momentum flux is given by the equation

$$M = 2\pi\rho \int_0^\infty U_x^2 r \, dr \tag{4}$$

According to Schlichting (ref. 1), the axial jet momentum must remain a constant at all distances downstream since a free jet has no external forces acting on it. Mathematically, the following relationship must be satisfied:

$$\frac{M}{M_o} = \int_0^\infty \left(\frac{U_x}{U_{max}}\right)^2 d\left[\left(\frac{r}{r_o}\right)^2\right] = 1 \tag{5}$$

This equation was checked by numerical integration using values determined from the velocity profiles presented in figures 8 and 9. The results of this integration are presented in figure 10. From figure 10 it can be seen that M/M_o remains essentially constant for both Reynolds numbers. This constant is 0.999 at the Reynolds number of 4751 and 0.786 at the Reynolds number of 1027, as determined by using an averaging procedure. The values of M/M_o are not unity since M_o is computed based on a theoretically uniform velocity profile at the nozzle exit. This deviation of the specified constants from unity is an indication of the relative uniformity of the incoming gaseous jet. As men-

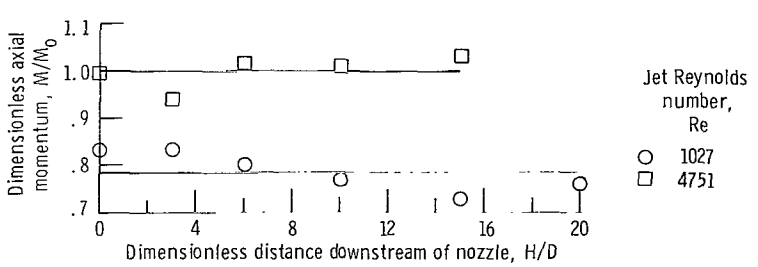

Figure 10. - Axial momentum as function of distance dowstream of nozzle.

tioned previously, it can be seen that the higher Reynolds numbers result in more uniform initial velocity profiles than do the lower Reynolds numbers.

Dependence of Centerline Velocity Decay on Jet Reynolds Number

Measurements of the centerline velocity were obtained at distances of 3, 6, 10, 15, 20, and 25 nozzle diameters downstream of the exit. Dimensionless centerline velocity as a function of dimensionless distance downstream of the nozzle with jet Reynolds number as a parameter is shown in figure 11. Reynolds numbers presented ranged from 155

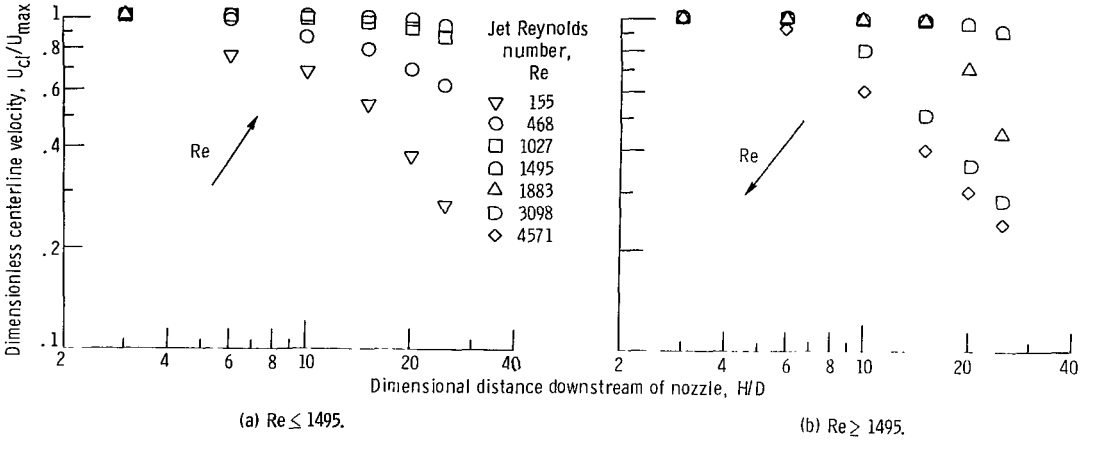

Figure 11. - Dependence of centerline velocity decay on jet Reynolds number.

to 4571. As the Reynolds number increased from 155 to 1495 (fig. 11(a)), the value of dimensionless centerline velocity at any given value of dimensionless distance downstream of the nozzle increased as the jet Reynolds number increased. For Reynolds numbers greater than 1495 (fig. 11(b)), the value of dimensionless centerline velocity at any given value of dimensionless distance downstream of the nozzle decreased as the Reynolds number increased.

Using the data presented in figure 11, the potential-core length as a function of jet Reynolds number can be determined. Previous investigators (refs. 2 and 8) have determined the length of the potential core by plotting, on log-log paper, the centerline velocity in the region of established flow against dimensionless distance downstream of the nozzle. The intersection of the line (having a slope of -1) representing the data and the horizontal line representing $U_{cl}/U_{max} = 1$ defined the potential-core length.

This criterion was arrived at by assuming that the velocity profiles in the region of flow establishment can be represented by a Gaussian distribution and that dynamic similarity exists throughout the flow field independent of the nozzle exit velocity. An examination of the data of this study, using this criterion, showed that this gave a reasonable representation of potential-core length for moderate to high values of jet Reynolds number (Re $\geq$ 3098) (see fig. 12).

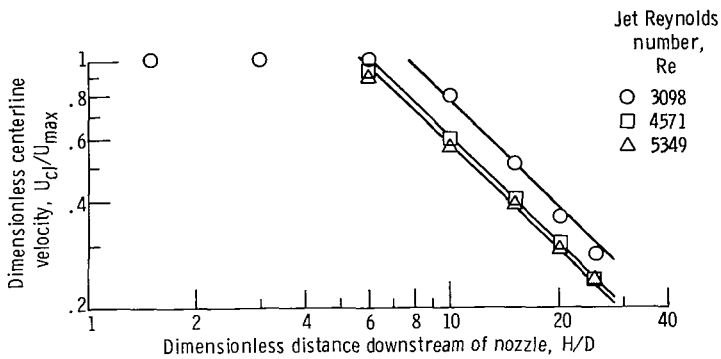

Figure 12. - Potential-core length data (ref. 8 criterion).

The intersection of these lines for the Reynolds numbers of 4571 and 5349 with the axis $U_{cl}/U_{max} = 1$ yielded potential-core lengths of order 6 and thus agrees with the results of reference 8. The potential-core length at the Reynolds number of 3098 was higher than that of reference 8 (probably due to the poor representation of the data using a faired slope of -1). The previously stated criterion is not valid for low-Reynolds-number flow. It is not surprising, therefore, that a fixed slope of -1 on log-log paper does not represent reference 8 data at low Reynolds numbers and would not represent the data of this study.

The potential-core length is defined physically as the distance over which the centerline velocity remains nearly constant and equal to the velocity at the nozzle exit. It appears reasonable to employ a definition of this type in specifying the potential-core length. In this study, the potential-core length is defined as the distance over which the centerline velocity was at least 95 percent of its initial value.

By using the data presented in figure 11 as well as data taken at Reynolds numbers of 717, 935, 1204, and 5349, lines were drawn between two adjacent values of H/D which were slightly less than and slightly greater than $U_{cl}/U_{max} = 0.95$. The value of H/D at which U_{cl}/U_{max} equalled 0.95 was defined as the potential-core length. By using this definition, dimensionless potential-core length as a function of jet Reynolds number was plotted in figure 13. Potential-core length increased with Reynolds number to a maximum of 21 nozzle diameters at a Reynolds number of approximately 1500 and then

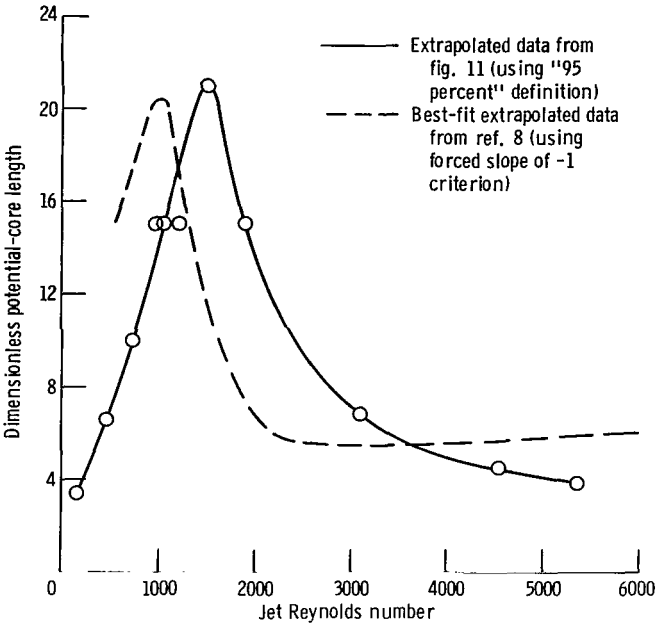

Figure 13. - Dependence of potential-core length on jet Reynolds number.

decreased with jet Reynolds number to a value of approximately 4 nozzle diameters as the jet Reynolds number increased to 5349.

An attempt was made to reexamine the data of reference 8 by using the "95 percent" definition of potential-core length. Unfortunately, the published data prevented an accurate determination of potential core by this method.

The variation in potential-core length, as presented in reference 8, is superimposed on figure 13. It is interesting to note that although different criteria were employed in obtaining the results, the behavior of potential-core length as a function of jet Reynolds number is similar. The shift in the peak of the two curves as well as the slight difference in core length at higher values of jet Reynolds number could conceivably have been caused by the different criteria or the difference in the nozzle designs employed in each study.

Jet Spreading

An indication of the magnitude of jet spreading can be obtained from an examination of the velocity profiles. The radial distance at which the dynamic pressure and, hence, axial velocity decreased to zero indicates the nominal boundary of the spreading jet.

The dimensionless jet radius at which the dynamic pressure decreases to zero is plotted as a function of the dimensionless distance downstream of the nozzle exit for jet Reynolds numbers of 468, 1027, 1883, 3098, and 4571 in figure 14. From lines faired through the data for each Reynolds number, half-angles of spread were calculated. The absolute values of these half-angles were found to be significantly affected by the jet Reynolds number. For the region of flow establishment, the half-angle of spread was found to vary from approximately 2^{o} to 7^{o}. In the region of established flow, the half-angle of spread was found to vary from approximately 2^{o} to 11^{o}.

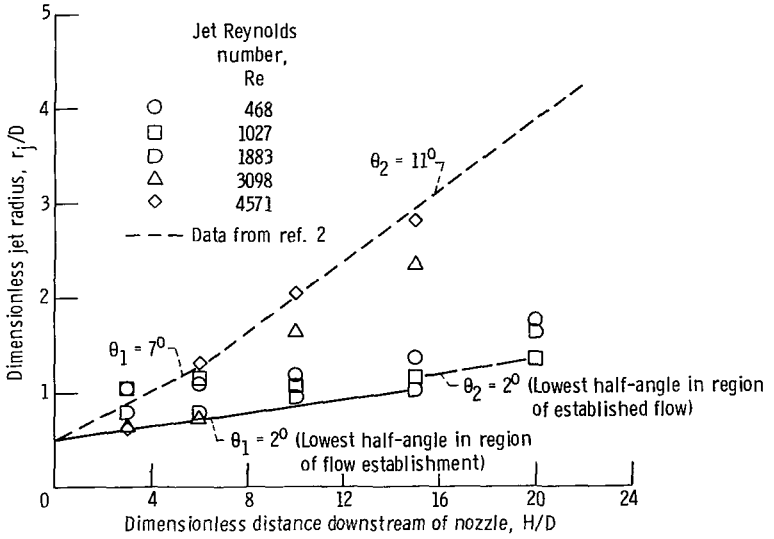

Figure 14. - Dimensionless jet radius as function of dimensionless distance from nozzle.

The variation of angle of spread with jet Reynolds number in the region of established flow was found to be similar to the variation of centerline velocity decay as presented in figure 11. Within the region of established flow, at any constant H/D, lower values of dimensionless axial jet velocity corresponded to higher values of the half-angle of spread. This was expected from conservation of axial jet momentum.

In figure 14, a short-dashed line represents the experimental data of reference 2, which were obtained for Reynolds numbers greater than 22 000. As seen, only the half-angle of spread at a jet Reynolds number of 4571 agrees favorably with the results of reference 2, the remaining half-angles of jet spreading being lower.

Mass Entrainment

The mass flow rate at the nozzle exit for a jet having an initially uniform velocity profile is given by

$$\dot{m}_o = \pi \rho r_o^2 U_{max} \tag{6}$$

At any distance downstream of the nozzle exit, the mass flow rate can be obtained by integrating the axial velocity profile. The resulting expression is as follows:

$$\dot{m} = 2\pi\rho \int_0^\infty U_x r \, dr \tag{7}$$

The dimensionless mass flow rate is, therefore, given as

$$\frac{\dot{m}}{\dot{m}_o} = \int_0^\infty \left(\frac{U_x}{U_{max}}\right) d\left(\frac{r}{r_o}\right)^2 \tag{8}$$

Since the initial velocity profiles for this study were not completely uniform, the values of $\dot{m}/\dot{m}_o$ as evaluated from equation (8) will not be unity at $H/D = 0$. It is desirable to normalize this mass flow ratio such that the plot of the dimensionless mass flow rate originates at 1 for an H/D of 0. Hence, equation (8) is multiplied by $\dot{m}_o/(\dot{m})_{H/D=0}$ to obtain the following expression:

$$\frac{\dot{m}}{(\dot{m})_{H/D=0}} = \frac{\dot{m}_o}{(\dot{m})_{H/D=0}} \left[\int_0^\infty \left(\frac{U_x}{U_{max}}\right) d\left(\frac{r}{r_o}\right)^2 \right] \tag{9}$$

Equation (8) was integrated numerically by using the velocity profiles presented in figures 8 and 9. It was then multiplied by $\dot{m}/(\dot{m})_{H/D=0}$ to obtain equation (9); the results are shown in figure 15. The entrained mass flux increased with distance downstream of the nozzle and was greater for the Reynolds number of 4571 than for the Reynolds number of 1027.

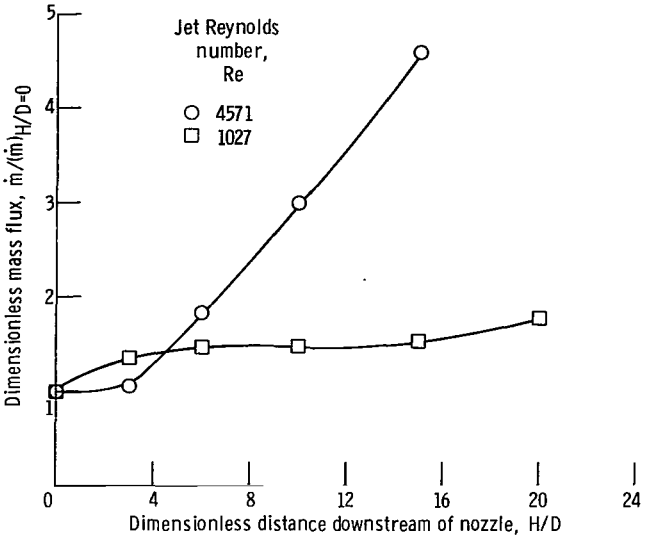

Figure 15. - Dependence of entrained mass flux on jet Reynolds number.

SUMMARY OF RESULTS

An experimental investigation was conducted to determine the flow characteristics of a circular free jet having an initially uniform velocity profile. The jet exited from a nozzle having the external shape of a tube and positioned vertically upward. The study was conducted over jet Reynolds numbers (based on nozzle diameter) ranging from 155 to 5349; and measurements were taken (where possible) at 0, 3, 6, 10, 15, 20, and 25 nozzle diameters from the nozzle exit. In all the tests, helium was the working fluid. This study yielded the following results:

1. The potential-core length (defined as the distance over which the centerline velocity was at least 95 percent of its initial value) was a function of the jet Reynolds number. The potential-core length increased to a maximum value at a Reynolds number of approximately 1500 and then decreased to approximately 4 nozzle diameters as the Reynolds number was increased toward 5349.

2. The potential-core length (using the "95 percent" criterion) reached a maximum value of 21 nozzle diameters at a jet Reynolds number of 1500, in contrast to the experimental results of Hrycak, Lee, Gauntner, and Livingood (using a -1 slope) in which a maximum value of approximately 21 nozzle diameters was obtained for the core length at a jet Reynolds number of 1000.

3. The half-angle of spread was a function of jet Reynolds number. This half-angle varied from 2° to 7° in the region of flow establishment (that region which begins at the nozzle and extends to the end of the potential core) and from approximately 2° to 11° in the region of established flow (that region beyond the potential core).

4. Within the region of established flow, at constant H/D, lower values of the dimensionless jet centerline velocity corresponded to higher values of the half-angle of spread.

5. The half-angles of spread at jet Reynolds numbers of 4571 and 5349 agree favorably with the experimental results presented by Albertson, Dai, Jensen, and Rouse.

6. The entrained mass flux increased with distance downstream of the nozzle and was greater for the Reynolds number of 4571 than for the Reynolds number of 1027.

7. The axial jet momentum flux remained essentially constant for a given value of jet Reynolds number at various distances downstream of the nozzle.

Lewis Research Center,
National Aeronautics and Space Administration,
Cleveland, Ohio, March 7, 1972,
113-31.

REFERENCES

1. Schlichting, Hermann (J. Kestin, trans.): Boundary Layer Theory. Fourth ed., McGraw-Hill Book Co., Inc., 1960.
2. Albertson, M. L.; Dai, Y. B.; Jensen, R. A.; and Rouse, Hunter: Diffusion of Submerged Jets. Am. Soc. Civil Eng. Proc., vol. 74, no. 10, Dec. 1948, pp. 1571-1596.
3. McNaughton, K. J.; and Sinclair, C. G.: Submerged Jets in Short Cylindrical Flow Vessels. J. Fluid Mech., vol. 25, pt. 2, June 1966, pp. 367-375.
4. Reynolds, A. J.: Observations of a Liquid-Into-Liquid Jet. J. Fluid Mech., vol. 14, pt. 4, Dec. 1962, pp. 552-556.
5. Andrade, E. N. da C.; and Tsien, L. C.: The Velocity-Distribution in a Liquid-Into-Liquid Jet. Proc. Phys. Soc., vol. 49, pt. 4, July 1937, pp. 381-391.
6. McKenzie, C. P.; and Wall, D. B.: Investigation of Jet Transition Phenomena. Rep. OR-9442, Martin Co. (AFOSR-68-1572, DDC No. AD-671977), June 1968.
7. Gauntner, James W.; Livingood, John N. B.; and Hrycak, Peter: Survey of Literature on Flow Characteristics of a Single Turbulent Jet Impinging on a Flat Plate. NASA TN D-5652, 1970.
8. Hrycak, Peter; Lee, David T.; Gauntner, James W.; and Livingood, John N. B.: Experimental Flow Characteristics of a Single Turbulent Jet Impinging on a Flat Plate. NASA TN D-5690, 1970.

9. Symons, Eugene P.; and Labus, Thomas L.: Experimental Investigation of an Axisymmetric Fully Developed Laminar Free Jet. NASA TN D-6304, 1971.

10. Miller, David R.; and Comings, Edward W.: Static Pressure Distribution in the Free Turbulent Jet. J. Fluid Mech., vol. 3, pt. 1, Oct. 1957, pp. 1-16.

11. Shapiro, Ascher H.: The Dynamics and Thermodynamics of Compressible Fluid Flow. Ronald Press Co., 1953.

12. Benedict, Robert P.: Fundamentals of Temperature, Pressure, and Flow Measurements. John Wiley & Sons, Inc., 1969.

13. Hurd, C. W.; Chesky, K. P.; and Shapiro, A. H.: Influence of Viscous Effects on Impact Tubes. J. Appl. Mech., vol. 20, no. 2, June 1953, pp. 253-256.

14. Lagerstrom, P. A.: Laminar Flow Theory. Theory of Laminar Flows. F. K. Moore, ed., Princeton Univ. Press, 1964, Sec. B.

15. Shames, Irving, H.: Mechanics of Fluids. McGraw-Hill Book Co., Inc., 1962.

NASA-Langley, 1972 —— 12 E-6801

"The aeronautical and space activities of the United States shall be conducted so as to contribute . . . to the expansion of human knowledge of phenomena in the atmosphere and space. The Administration shall provide for the widest practicable and appropriate dissemination of information concerning its activities and the results thereof."

—NATIONAL AERONAUTICS AND SPACE ACT OF 1958

NASA SCIENTIFIC AND TECHNICAL PUBLICATIONS

TECHNICAL REPORTS: Scientific and technical information considered important, complete, and a lasting contribution to existing knowledge.

TECHNICAL NOTES: Information less broad in scope but nevertheless of importance as a contribution to existing knowledge.

TECHNICAL MEMORANDUMS: Information receiving limited distribution because of preliminary data, security classification, or other reasons.

CONTRACTOR REPORTS: Scientific and technical information generated under a NASA contract or grant and considered an important contribution to existing knowledge.

TECHNICAL TRANSLATIONS: Information published in a foreign language considered to merit NASA distribution in English.

SPECIAL PUBLICATIONS: Information derived from or of value to NASA activities. Publications include conference proceedings, monographs, data compilations, handbooks, sourcebooks, and special bibliographies.

TECHNOLOGY UTILIZATION PUBLICATIONS: Information on technology used by NASA that may be of particular interest in commercial and other non-aerospace applications. Publications include Tech Briefs, Technology Utilization Reports and Technology Surveys.

Details on the availability of these publications may be obtained from:

SCIENTIFIC AND TECHNICAL INFORMATION OFFICE

NATIONAL AERONAUTICS AND SPACE ADMINISTRATION

Washington, D.C. 20546